Macroscopic yielding in jammed solids is accompanied by a nonequilibrium first-order transition in particle trajectories

Takeshi Kawasaki[1,2] and Ludovic Berthier[1]

[1]*Laboratoire Charles Coulomb, UMR 5221 CNRS, Montpellier, France*
[2]*Department of Physics, Nagoya University, Nagoya 464-8602, Japan*

We use computer simulations to analyze the yielding transition during large-amplitude oscillatory shear of a simple model for soft jammed solids. Simultaneous analysis of global mechanical response and particle-scale motion demonstrates that macroscopic yielding, revealed by a smooth crossover in mechanical properties, is accompanied by a sudden change in the particle dynamics, which evolves from nondiffusive motion to irreversible diffusion as the amplitude of the shear is increased. We provide numerical evidence that this sharp change corresponds to a nonequilibrium first-order dynamic phase transition, thus establishing the existence of a well-defined microscopic dynamic signature of the yielding transition in amorphous materials in oscillatory shear.

I. INTRODUCTION

A major effort in soft condensed matter physics concerns the design of materials with well-controlled mechanical properties [1]. Rheology thus represents a central probe, and oscillatory shear measurements at finite frequency ω are among the most commonly performed mechanical tests [2]. In this approach, a harmonic deformation is applied and the stress response measured or vice versa. In the linear regime, the complex shear modulus $G^*(\omega) = G'(\omega) + iG''(\omega)$ provides information about the nature and strength of the material at a given frequency [3], while microscopic relaxation processes can be probed by varying the frequency. At larger amplitude, nonlinear mechanical properties are accessed.

This approach is well suited for amorphous materials, which often display nontrivial response spectra in the linear regime where they behave as soft elastic solids but flow as the amplitude of the forcing is increased beyond a "yielding" limit [4–6]. Whereas the storage modulus $G'(\omega)$ dominates the elastic response at small deformation amplitude, irreversible plastic deformations occur after yielding where the loss modulus $G''(\omega)$ dominates instead. Oscillatory shear experiments have been performed in a wide range of soft condensed matter systems across yielding, such as granular particles [7–11], emulsions [12–15], colloidal suspensions [16–18], and gels [19], as well as in computer simulations [20–24].

In experiments, the change from elastic to plastic response in macroscopic mechanical properties is often described as a "yielding transition," even though yielding appears as a smooth crossover whose location cannot be unambiguously defined [25]. Interestingly, recent experiments have provided evidence that this macroscopic crossover corresponds to a qualitative change in particle trajectories [9,11,12,18,26–28]. As expected physically, particles are essentially arrested in the undeformed solid but can diffuse due to irreversible plastic rearrangements occurring at larger amplitude. There is, however, no consensus about the nature of this crossover, which has been described either as a smooth change [10], as a relatively sharp crossover [12], or as a continuous nonequilibrium phase transition [18]. The last conclusion builds a qualitative analogy with the continuous irreversibility transition observed in low-density suspensions [7,8,29], which has been actively studied in computer simulations [23,24] and attempts to borrow concepts

from the field of nonequilibrium phase transitions [30–32]. In addition recent experiments argue that yielding corresponds to a change in the microstructure of the system [27], by opposition to the dynamic properties discussed here. A clear connection between these microscopic changes and the macroscopic rheology is lacking.

Here we use a model of a jammed material composed of non-Brownian repulsive spheres to investigate the nature of the yielding transition at the particle-scale level, in the simple situation where thermal fluctuations and hydrodynamic forces play no role. We reproduce standard mechanical signatures of macroscopic yielding under oscillatory shear and obtain two key results regarding particle trajectories. First, we show that the onset of particle diffusion in steady state is extremely sharp and occurs at a well-defined shear amplitude, which unambiguously locates the yielding transition. Second, we find that particle diffusivity emerges discontinuously at yielding, thus demonstrating that yielding corresponds to a nonequilibrium first-order phase transition. These findings differ qualitatively from earlier suggestions of a continuous irreversibility transition [18,24] but seem to agree very well with recent experimental findings [10,12]. We also show that this transition is dynamic in nature and is not accompanied by discontinuous structural changes.

II. MODEL AND NUMERICAL TECHNIQUES

We consider soft repulsive non-Brownian particles in a simple shear flow geometry. We perform standard overdamped Langevin dynamics simulations of a well-known model of harmonic particles in three dimensions [33,34], using an equimolar binary mixture of small and large particles with diameter ratio 1.4. The equations of motion read

$$\xi_s \left[\frac{\partial \vec{r}_i}{\partial t} - \dot{\gamma}(t) y_i(t) \vec{e}_x \right] + \sum_j \frac{\partial U(r_{ij})}{\partial \vec{r}_{ij}} = \vec{0}, \quad (1)$$

where ξ_s is a friction coefficient, $\vec{r}_{ij} = (x_{ij}, y_{ij}, z_{ij}) = (x_j - x_i, y_j - y_i, z_j - z_i)$, $\vec{e}_x = (1,0,0)$, and $\dot{\gamma}(t)$ is the shear rate. For particles i and j having diameters a_i and a_j, the pair potential reads $U(r_{ij}) = \frac{\epsilon}{2}(1 - r_{ij}/a_{ij})^2 \Theta(a_{ij} - r_{ij})$, where ϵ is an energy scale, $a_{ij} = (a_i + a_j)/2$, a denotes the diameter

of small particles, and $\Theta(x)$ is the Heaviside function. The unit length is a, the unit time $\tau_0 = a^2 \xi_s / \epsilon$, the unit energy ϵ, and so the unit stress is ϵ / a^3.

We apply a harmonic deformation using Lees-Edwards periodic boundary conditions [34], the strain evolving as $\gamma(t) = \gamma_0 [1 - \cos(\omega t)]$, where γ_0 is the amplitude of the imposed shear strain and $\omega = 2\pi / T$ is the frequency of the oscillation. The period T is chosen very large to be close to a quasistatic protocol; we use $T = 10^4 \tau_0$. We have checked that our results do not qualitatively depend on this choice. We work at constant packing fraction $\varphi = 0.80$, much above the jamming density $\varphi_J \simeq 0.647$ [35]. We checked that our results are representative of the entire jammed phase, $\varphi > \varphi_J$, but yielding could be more complicated in the limit $\varphi \to \varphi_J$ where the system loses rigidity [12]. The different regime $\varphi < \varphi_J$, where a yield stress does not exist, was analyzed previously [29]. We solve Eq. (1) with a modified Euler algorithm [34] using a discretization time step $\Delta t = 0.1 \tau_0$. Numerical stability and accuracy were carefully checked. To investigate finite-size effects, we perform simulations with four different sizes, $N = 300$, 1000, 3000, and 10 000, where N is the total number of particles. All simulations start from fully random configurations. We analyze both the transient regime after shear is started and steady-state measurements. To improve the statistics, we perform at least four independent runs for each pair (γ_0, N).

At the macroscopic level, our main observable is the time-dependent response of the xy component of the shear stress, defined by the usual Irving-Kirkwood formula [34]: $\sigma(t) = -\frac{1}{V} \sum x_{ij} F_{ij}^y$, where V is the volume and F_{ij}^y represents the y component of the force F_{ij}. The kinetic part of the stress is fully negligible in the present situation of low-frequency oscillatory shear. To analyze the rheological response in steady state, we fit the time series of the shear stress to a sinusoidal form,

$$\sigma(t) = -\sigma_0 \cos(\omega t + \delta), \qquad (2)$$

where σ_0 is the amplitude of the first harmonics at frequency ω, and δ is the phase difference between strain and stress. In practice, σ_0 and δ are obtained by fitting Eq. (2) to steady-state data lasting about $100T$. Alternatively, we can transform the two parameters (σ_0, δ) into the more conventional quantities $G'(\omega)$ and $G''(\omega)$ using

$$G'(\omega) + \mathrm{i} G''(\omega) = \frac{\sigma_0}{\gamma_0} e^{\mathrm{i}\delta}. \qquad (3)$$

III. SMOOTH CROSSOVER IN MACROSCOPIC RHEOLOGY

In Fig. 1(a) we show the evolution with the strain amplitude γ_0 of the storage and loss moduli at fixed frequency ω measured in steady state. At very low γ_0, G' dominates the response, $G'/G'' \approx 10$, indicating that the system responds in the linear regime as a soft elastic solid. As γ_0 is increased, the moduli first evolve slowly for $\gamma_0 < 0.1$, where little plastic rearrangements are produced. As γ_0 increases further, we observe a crossing of G' and G'' at $\gamma_\times \approx 0.15$ (dashed lines), so that dissipation dominates $\gamma_0 > \gamma_\times$. These mechanical properties reproduce well-known behavior [1,2] and validate our numerical approach. We notice further that they display
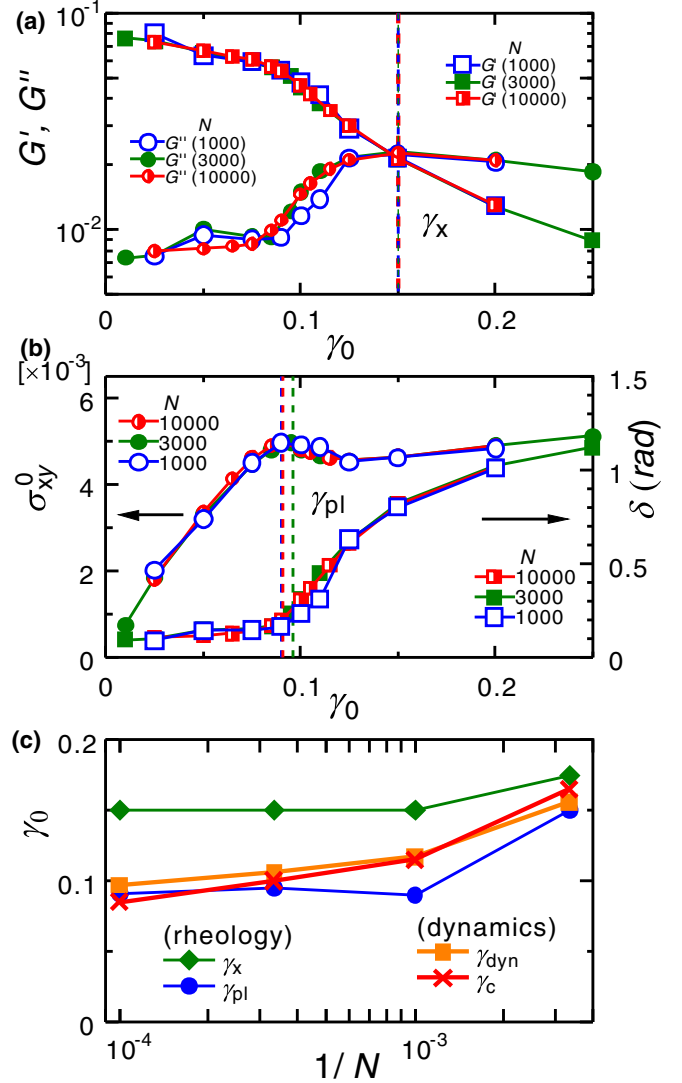

FIG. 1. (a) Evolution of storage and loss moduli [Eq. (3)] with strain amplitude for different system sizes. The crossing of G' and G'' at $\gamma_\times$ (dashed lines) defines a characteristic strain scale. (b) Evolution of amplitude and phase of the stress [Eq. (2)] with strain amplitude. The amplitude has a maximum at γ_{pl} (dashed lines). (c) System size dependence of all characteristic strain amplitudes.

virtually no finite-size effects. In this representation, $\gamma_\times \approx 0.15$ appears as the most relevant strain scale to characterize yielding, although a smooth crossover can be qualitatively detected near $\gamma_0 \approx 0.1$, where the γ_0 dependence of the moduli becomes somewhat steeper.

In Fig. 1(b) we replot this rheological evolution in the alternative representation offered by (σ_0, δ). At small γ_0, the phase δ is very small while the stress amplitude increases linearly, $\sigma_0 \approx G' \gamma_0$, as expected for reversible elastic deformations in a solid. Near $\gamma_0 \approx 0.1$ two changes are observed. First, σ_0 ceases to be linear and displays an overshoot when γ_0 is increased, signaling that plastic events take place. We define the onset of plastic events, γ_{pl}, as the location of the stress overshoot [dashed lines in Fig. 1(b)]. Our interpretation for γ_{pl} is reinforced by the evolution of the phase δ in Fig. 1(b), which grows steadily above γ_{pl}, indicating the onset of dissipation.

Note that the crossing of G' and G'' at $\gamma_\times$ has no obvious relevance in this representation where it simply corresponds, by definition, to the strain scale where $\delta = \pi/4$. In Fig. 1(c) we confirm that γ_{pl} and $\gamma_\times$ display virtually no system size dependence, but that they differ quantitatively.

Whereas $\gamma_\times$ is frequently quoted as "the" yielding point in the literature, a stress overshoot also serves to identify yielding in shear-start experiments [25]. A stress overshoot is reported in some oscillatory shear experiments [19] but is absent in others [12,13]. A possible explanation is that experiments are typically performed at somewhat larger frequencies, where additional contributions to the shear stress (lubrication forces, hydrodynamic effects) might hide this behavior. In addition, we have confirmed that the overshoot disappears and is replaced by a monotonic increase seen in experiments [13] when we use a substantially larger frequency, typically $\omega > 10^{-3}$. We emphasize that the presence of the dynamic transition discussed below is independent of the existence of the stress overshoot reported in Fig. 1(b).

IV. SHARP TRANSITION IN MICROSCOPIC DYNAMICS

We now turn to the evolution of single particle dynamics. A first natural dynamic observable is the averaged particle displacement after one deformation cycle [12,24],

$$\Delta r(t,T) = \frac{1}{N} \sum_j |\vec{r}_j(t+T) - \vec{r}_j(t)|, \qquad (4)$$

where t is the time since shear is applied. In Fig. 2(a) we show how $\Delta r(t,T)$ evolves in the transient regime for various amplitudes of the applied deformation. For small γ_0, particle displacements decay rapidly to zero. In the elastic solid at small amplitude, there are rare rearrangements taking place before the system settles near a stable energy minimum where particles have nearly periodic motion (or quasiperiodic motion with a period that is a multiple of T, as reported previously [23,36]). As γ_0 is increased, it takes more and more time for $\Delta r(t,T)$ to eventually vanish. When γ_0 is larger than $\gamma \sim 0.095$, the average particle displacement never vanishes in the explored time window, but instead fluctuates around a well-defined finite value, which increases with γ_0. This regime corresponds to irreversible, nonperiodic particle trajectories. In Fig. 2(b) we plot the time-averaged displacement for one cycle $\langle \Delta r(T) \rangle$ in steady states for various strain amplitudes and system sizes. From $\langle \Delta r(T) \rangle$, a very clear discontinuous jump is observed between the irreversible and reversible states near γ_c. Very close to the transition, the displacements exhibit fluctuations around a well-defined value both above and below γ_c. Whereas these fluctuations are infinitely long-lived above γ_c, they are only metastable below γ_c, before the system finds a reversible state where the displacements become very small. We report the value of $\langle \Delta r(T) \rangle$ for $N = 10\,000$ for these metastable states in Fig. 2(b). Overall, these fluctuations appear qualitatively distinct from the algebraic decay observed close to continuous irreversibility transitions [8] and are much closer to the phenomenology observed near discontinuous, first-order phase transitions where metastable phases can be observed over long times. In particular, it appears impossible to
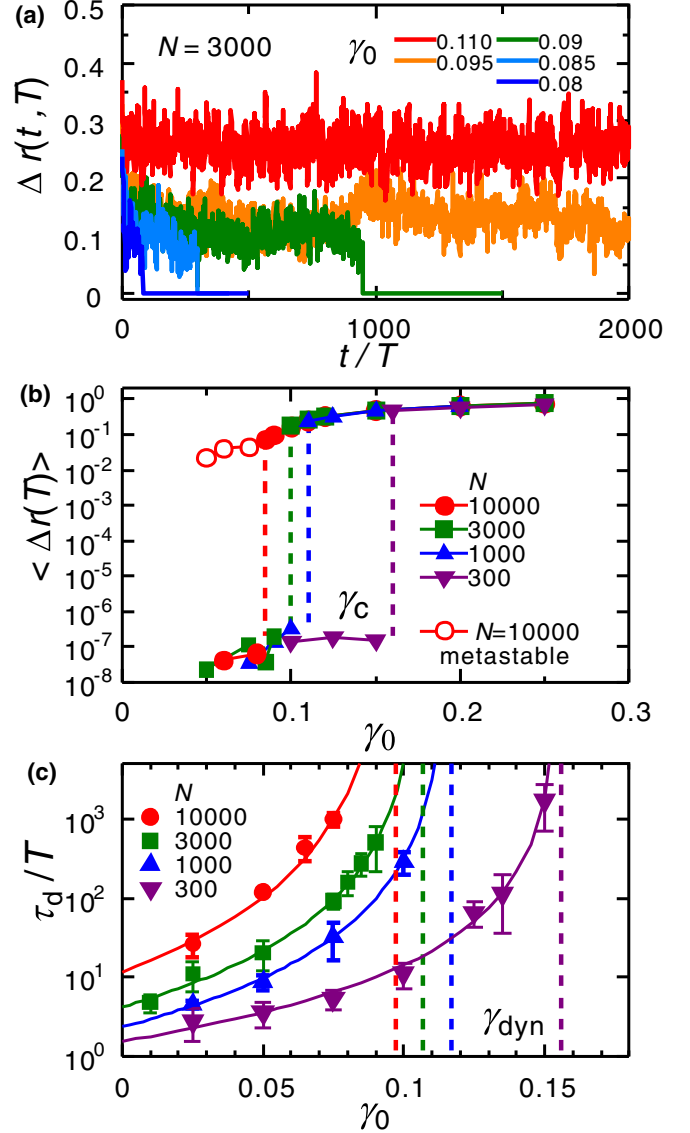

FIG. 2. (a) Transient evolution of particle displacement $\Delta r(t,T)$ [Eq. (4)] for various strain amplitudes for $N = 3000$. For $\gamma_0 \lesssim 0.090$, the displacements drop to zero after a time scale τ_d. (b) The time-averaged displacement for one cycle $\langle \Delta r(T) \rangle$ for various strain amplitudes and system sizes. The stable and the metastable data are plotted with filled and open symbols, respectively. The vertical dashed lines indicate γ_c for each system size. (c) The average τ_d diverges algebraically, $\tau_d \sim (\gamma_{dyn} - \gamma_0)^{-\alpha}$, interpreted as the diverging lifetime of a metastable state near a discontinuous phase transition. The vertical dashed lines indicate γ_{dyn} for each system size.

describe the decrease of $\langle \Delta r(T) \rangle$ with a continuous vanishing at the critical value of γ_{dyn}.

Stronger evidence of such a phase transition is obtained from the evolution of the average lifetime of the metastable irreversible phase τ_d, as depicted in Fig. 2(c) for various system sizes. These data confirm that τ_d increases rapidly close to $\gamma_0 \approx 0.1$. For larger γ_0, trajectories remain irreversible. By contrast to the rheology, a clear system size dependence is observed, and larger systems take more time to settle in a global energy
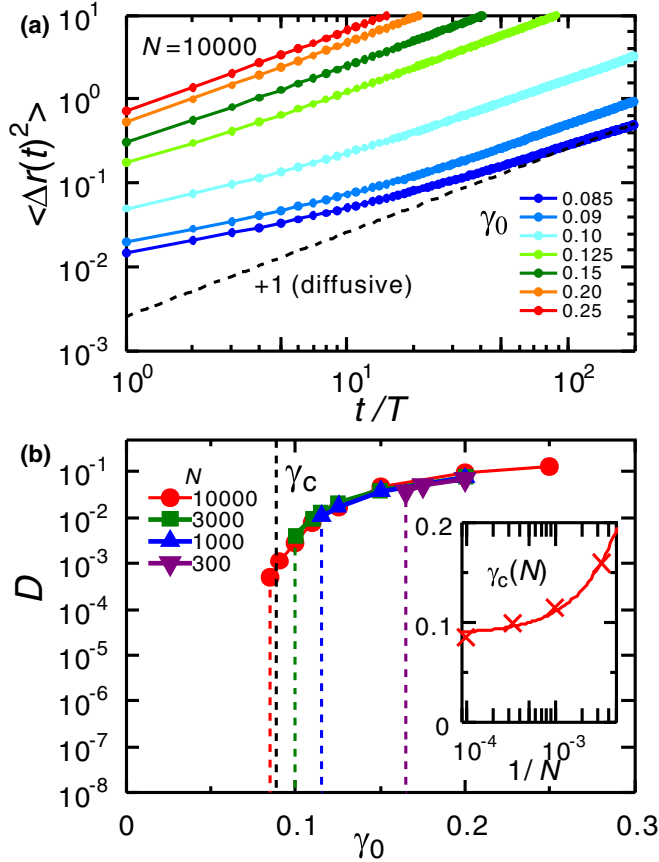
FIG. 3. (a) Mean-squared displacements [Eq. (5)] for $N = 10^4$ and various strain amplitude become diffusive at long time when $\gamma_0 \geqslant \gamma_c \approx 0.085$. (b) The diffusion constant D decreases modestly as γ_0 decreases towards a critical value γ_c where it drops discontinuously to zero. The vertical dashed lines indicate γ_c for each system size, and the black one represents the large-N extrapolation of $\gamma_c \approx 0.0885$ performed in the inset.

minimum. A diverging lifetime is typically observed close to nonequilibrium phase transitions [8,30,31] and was reported previously [23,24]. Such divergence is expected for either a continuous or discontinuous transition (see Refs. [37,38] for recent examples). Solid lines in Fig. 2(c) represent an empirical fit, $\tau_d \sim (\gamma_{\mathrm{dyn}} - \gamma_0)^{-\alpha}$, with $\alpha \approx 2.1$–3.0 [39], suggestive of a divergence of τ_d when approaching the dynamic transition at γ_{dyn}. We notice that finite size effects can be felt even when the system is not very close to the critical value, such that we cannot observe the expected saturation of τ_d to a finite value as $N \to \infty$. The system size dependence of γ_{dyn} reported in Fig. 1(a) is very modest and seems to extrapolate to a finite value, $\gamma_{\mathrm{dyn}} \approx 0.095$, as $N \to \infty$.

We now characterize the steady-state irreversible dynamics at large γ_0 using the mean-squared displacement,

$$\langle \Delta r(t)^2 \rangle = \frac{1}{N} \left\langle \sum_{j=1}^{N} |\vec{r}_j(t) - \vec{r}_j(0)|^2 \right\rangle, \quad (5)$$

where the brackets indicate a time average. The results are displayed in Fig. 3(a) for $N = 10^4$, for time delays commensurate with the period. The dynamics is diffusive at

long times, $\langle \Delta r(t)^2 \rangle \sim 6Dt$, where D is the diffusion constant. We represent D (in units of a^2/T) for various γ_0 and N in Fig. 3(b). As expected, $D = 0$ below a critical value γ_c, corresponding to the phase characterized by quasiperiodic particle trajectories, and it increases with γ_0 above γ_c. Both D and $\Delta r(t, T)$ in Eq. (4) could serve as order parameters for the transition. By measuring γ_c for various system sizes, we observe a modest change with system size [see inset of Fig. 3(b)] suggestive of a finite limit $\gamma_c \approx 0.0885$ for $N \to \infty$. The functional form of our extrapolation should be confirmed by additional larger scale simulations.

A striking finding in Fig. 3(b) is the finite amplitude of the diffusion constant at the transition. Near continuous irreversibility transitions, D decreases by several orders of magnitude and scales algebraically as γ_c is approached from above [7,40]. We observe instead a modest decrease of D, followed by a sudden jump to zero, which is robust against finite-size effects. In particular we find that diffusive behavior also persists for a finite amount of time below in the reversible phase, as also described above for the one-cycle particle displacement $\langle \Delta r(T) \rangle$. It is more difficult, however, to measure D in this region, because a careful determination of D requires taking the long-time limit, which is not possible by construction in the metastable region. We conclude therefore that the discontinuous behavior of D in Fig. 3(b) appears less convincing than the one of $\langle \Delta r(T) \rangle$ shown in Fig. 2(b), but the overall phenomenology reported in this work appears inconsistent with a continuous transition.

V. NO CHANGE IN MICROSCOPIC STRUCTURE

It was recently argued that the yielding transition in oscillatory shear can be detected through the static structure of the system [27]. Such a behavior would differ qualitatively from our conclusion that yielding is revealed through the dynamic evolution of the system. Our analysis of the pair correlation function across the yielding transition did not reveal any change in the static properties of the system in the two phases, which seems to contradict the results of Ref. [27]. To reinforce this conclusion, we have measured the exact same quantity that was detected experimentally. In detail, we resolve the radial dependence of the static structure factor $S(\vec{q}) = \frac{1}{N} \langle \rho(\vec{q})\rho(-\vec{q}) \rangle$ in the (x, z) plane [27], where $\rho(\vec{q})$ is the Fourier component of the density at wave vector $\vec{q}$. Thus we define the angle α from $\tan \alpha = (q_z/q_x)$ and follow the α dependence of the static structure, as proposed in Ref. [27].

To obtain statistically reliable data close to the dynamic transition, we perform an extensive time average over 100 well-separated times for the diffusive phase at $\gamma_0 = 0.12$. For the nondiffusive phase at $\gamma_0 = 0.10$, time averages are not useful, and we obtain instead 100 independent configurations starting from independent initial conditions. Error bars are defined from the resulting sample-to-sample fluctuations. Because the stress is close to a sinusoidal form, we measure the structure either when the stress is zero ("undeformed" states) and when it is maximal $\sigma(t) = \pm \sigma_0$ ("deformed" states). Thus, we obtain four measures of the structure at two shear amplitudes, for both deformed and undeformed states.
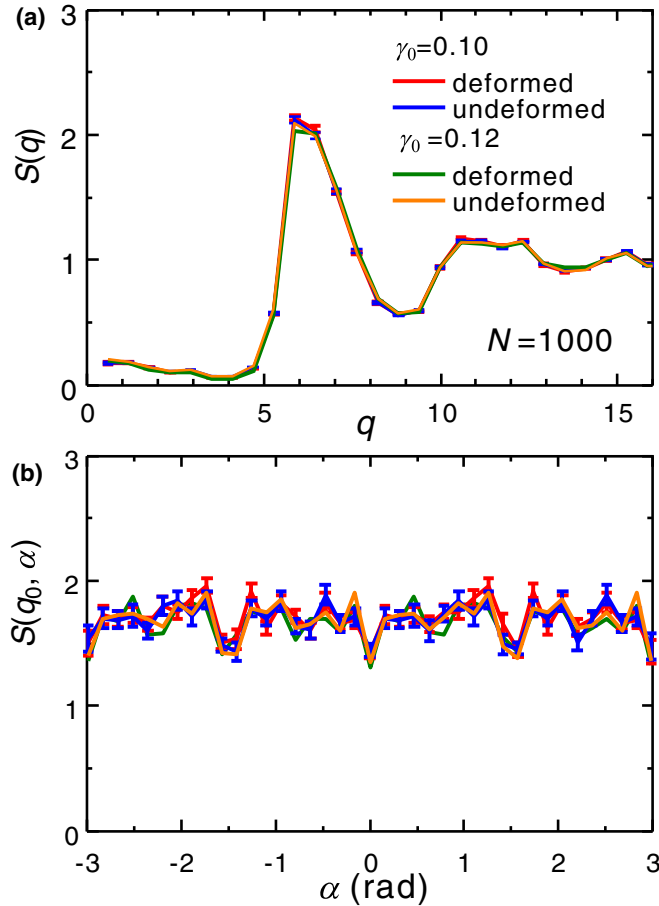
FIG. 4. Averaged static structure factors for "deformed" (when the stress is maximal) and undeformed (when the stress is zero) states in the reversible phase at $\gamma_0 = 0.10$ and in the diffusive phase at $\gamma_0 = 0.12$, for $N = 10^3$. (a) Wave-vector dependence of the structure with spherical average over all directions. (b) Angular dependence of the structure factor for $|\vec{q}|$ near the first peak as a function of the angle α defined the (x, z) components of $\vec{q}$. Error bars are shown for $\gamma_0 = 0.10$, to indicate that our relative resolution is very good (about 2%).

In Fig. 4(a) we show the q dependence of the averaged structure factor $S(q = |\vec{q}|)$ for these four cases and for $N = 1000$. We observe that neither the particle reversibility nor the deformation seem to affect much the structure factor. We now resolve the angular dependence of $S(q_0, \alpha)$ using wave vectors in the (x, z) plane having an amplitude close to the first peak in the range $q_0 = 5.9 - 7.0$. In Fig. 4(b) we show that the α dependence of the structure factor for the four situations defined above is essentially nonexistent. Importantly, we do not observe any difference for reversible and irreversible regimes across yielding. In particular we do not observe the oscillations that were detected in the experiments for the arrested phase. Furthermore, we also checked that average values of other static quantities (such as the energy density and pair correlation functions) are similarly insensitive to the underlying dynamic transition. These conclusions contrast with the results in Ref. [27], which are perhaps due to the larger shear rates employed in the experiment. Another major contradiction with that work is our finding that yielding does not correspond to the crossing point of G' and G''. Our results show that yielding is best interpreted as a loss of reversibility in the particle trajectories, which is a purely dynamical concept.

VI. CONCLUSION

Together, our results suggest that the yielding transition of jammed solids under large-amplitude oscillatory shear is accompanied by a first-order nonequilibrium phase transition, rather than a continuous one. It marks the abrupt emergence of irreversible nonaffine particle motion. The characteristic strain amplitudes obtained from rheology ($\gamma_\times$, γ_{pl}) and from microscopic dynamics (γ_{dyn}, γ_c) are compiled in Fig. 1(c). To a good approximation, we find that $\gamma_{pl} \approx \gamma_{dyn} \approx \gamma_c$, whereas $\gamma_\times$ is significantly larger, corresponding to a large amount of dissipated energy. The dynamic phase transition revealed by the discontinuous evolution of single-particle dynamics produces a smooth crossover in mechanical properties at a critical strain amplitude that appears unrelated to the crossing of $G'(\omega)$ and $G''(\omega)$. Our conclusions contrast with earlier claims of a continuous transition [18,24] but appear in very good agreement with observations in a sheared emulsion [12]. We hope our study will trigger further work in a broader variety of numerical and experimental systems to fully establish its generality.

[1] R. G. Larson, *The Structure and Rheology of Complex Fluids* (Oxford University Press, Oxford, 1999).

[2] K. Hyun, M. Wilhelm, C. O. Klein, K. S. Cho, J. G. Nam, K. H. Ahn, S. J. Lee, R. H. Ewoldt, and G. H. McKinley, A review of nonlinear oscillatory shear tests: Analysis and application of large amplitude oscillatory shear (LAOS), Prog. Polym. Sci. **36**, 1697 (2011).

[3] J. R. de Bruyn and F. K. Oppong, Rheological and microrheological measurements of soft condensed matter, in *Experimental and Computational Techniques in Soft Condensed Matter Physics*, edited by J. Olafsen (Cambridge University Press, Cambridge, 2010), p. 147.

[4] P. Sollich, Rheological constitutive equation for a model of soft glassy materials, Phys. Rev. E **58**, 738 (1998).

[5] L. Berthier and G. Biroli, Theoretical perspective on the glass transition and amorphous materials, Rev. Mod. Phys. **83**, 587 (2011).

[6] N. Perchikova and E. Bouchbinder, Variable-amplitude oscillatory shear response of amorphous materials, Phys. Rev. E **89**, 062307 (2014).

[7] D. J. Pine, J. P. Gollub, J. F. Brady, and A. M. Leshansky, Chaos and threshold for irreversibility in sheared suspensions, Nature (London) **438**, 997 (2005).

[8] L. Corté, P. M. Chaikin, J. P. Gollub, and D. J. Pine, Random organization in periodically driven systems, Nature Phys. **4**, 420 (2008).

[9] N. C. Keim and P. E. Arratia, Mechanical and Microscopic Properties of the Reversible Plastic Regime in a 2D Jammed Material, Phys. Rev. Lett. **112**, 028302 (2014).

[10] N. C. Keim and P. E. Arratia, Yielding and microstructure in a 2D jammed material under shear deformation, Soft Matter **9**, 6222 (2013).

[11] S. Slotterback, M. Mailman, K. Ronaszegi, M. van Hecke, M. Girvan, and W. Losert, Onset of irreversibility in cyclic shear of granular packings, Phys. Rev. E **85**, 021309 (2012).

[12] E. D. Knowlton, D. J. Pine, and L. Cipelletti, A microscopic view of the yielding transition in concentrated emulsions, Soft Matter **10**, 6931 (2014).

[13] T. G. Mason, J. Bibette, and D. A. Weitz, Yielding and flow of monodisperse emulsions, J. Colloid Interface Sci. **179**, 439 (1996).

[14] P. Hébraud, F. Lequeux, and J. P. Munch, Yielding and rearrangements in disordered emulsions, Phys. Rev. Lett. **78**, 4657 (1997).

[15] J. Clara-Rahola, T. A. Brzinski, D. Semwogerere, K. Feitosa, J. C. Crocker, J. Sato, V. Breedveld, and E. R. Weeks, Affine and non-affine motions in sheared polydisperse jammed emulsions, Phys. Rev. E **91**, 010301(R) (2015).

[16] G. Petekidis, A. Moussaid, and P. N. Pusey, Rearrangements in hard-sphere glasses under oscillatory shear strain, Phys. Rev. E **66**, 051402 (2002).

[17] N. Koumakis, J. F. Brady, and G. Petekidis, Complex Oscillatory Yielding of Model Hard-Sphere Glasses, Phys. Rev. Lett. **110**, 178301 (2013).

[18] K. H. Nagamanasa, S. Gokhale, A. K. Sood, and R. Ganapathy, Experimental signatures of a nonequilibrium phase transition governing the yielding of a soft glass, Phys. Rev. E **89**, 062308 (2014).

[19] M. C. Rogers, K. Chen, L. Andrzejewski, S. Narayanan, and S. Ramakrishnan, Echoes in x-ray speckles track nanometer-scale plastic events in colloidal gels under shear, Phys. Rev. E **90**, 062310 (2014).

[20] L. Mohan, C. Pellet, M. Cloitre, and R. Bonnecaze, Local mobility and microstructure in periodically sheared soft particle glasses and their connection to macroscopic rheology, J. Rheol. **57**, 1023 (2013).

[21] J. M. Brader, M. Siebenburger, M. Ballauff, K. Reinheimer, M. Wilhelm, S. J. Frey, F. Weysser, and M. Fuchs Nonlinear response of dense colloidal suspensions under oscillatory shear: Mode-coupling theory and Fourier transform rheology experiments, Phys. Rev. E **82**, 061401 (2010).

[22] N. V. Priezjev, Heterogeneous relaxation dynamics in amorphous materials under cyclic loading, Phys. Rev. E **87**, 052302 (2013).

[23] I. Regev, T. Lookman, and C. Reichhardt, Onset of irreversibility and chaos in amorphous solids under periodic shear, Phys. Rev. E **88**, 062401 (2013).

[24] D. Fiocco, G. Foffi, and S. Sastry, Oscillatory athermal quasistatic deformation of a model glass, Phys. Rev. E **88**, 020301(R) (2013).

[25] D. Bonn, J. Paredes, M. M. Denn, L. Berthier, T. Divoux, and S. Manneville, Yield stress materials in soft condensed matter, arXiv:1502.05281.

[26] V. Chikkadi, D. M. Miedema, M. T. Dang, B. Nienhuis, and P. Schall, Shear Banding of Colloidal Glasses: Observation of a Dynamic First-Order Transition, Phys. Rev. Lett. **113**, 208301 (2014).

[27] D. V. Denisov, M. T. Dang, B. Struth, A. Zaccone, G. H. Wegdam, and P. Schall, Sharp symmetry-change marks the mechanical failure transition of glasses, Sci. Rep. **5**, 14359 (2015).

[28] I. Regev, J. Weber, C. Reichhardt, K. A. Dahmen, and T. Lookman, Reversibility and criticality in amorphous solids, Nature Comm. **6**, 8805 (2015).

[29] C. F. Schreck, R. S. Hoy, M. D. Shattuck, and C. S. O'Hern, Particle-scale reversibility in athermal particulate media below jamming, Phys. Rev. E **88**, 052205 (2013).

[30] J. A. Acebron, L. L. B. Conrad, J. P. Vicente, F. Ritort, and R. Spigler, The Kuramoto model: A simple paradigm for synchronization phenomena, Rev. Mod. Phys. **77**, 137 (2005).

[31] H. Hinrichsen, Nonequilibrium critical phenomena and phase transitions into absorbing states, Adv. Phys. **49**, 815 (2000).

[32] M. Henkel, H. Hinrichsen, and S. Lubeck, *Non-equilibrium Phase Transitions I: Absorbing Phase Transitions* (Springer, Heidelberg, 2008).

[33] D. J. Durian, Foam Mechanics at the Bubble Scale, Phys. Rev. Lett. **75**, 4780 (1995).

[34] M. Allen and D. Tildesley, *Computer Simulation of Liquids* (Oxford University Press, Oxford, 1987).

[35] T. Kawasaki, D. Coslovich, A. Ikeda, and L. Berthier, Diverging viscosity and soft granular rheology in non-Brownian suspensions, Phys. Rev. E **91**, 012203 (2015).

[36] M. Lundberg, K. Krishan, N. Xu, C. S. O'Hern, and M. Dennin, Reversible plasticity in amorphous materials, Phys. Rev. E **77**, 041505 (2008).

[37] C. E. Fiore, Minimal mechanism leading to discontinuous phase transitions for short-range systems with absorbing states, Phys. Rev. E **89**, 022104 (2014).

[38] S. L. Y. Xu and J. M. Schwarz, Contact processes in crowded environments, Phys. Rev. E **88**, 052130 (2013).

[39] The exponent α obtained in each system size is the following: $\alpha = -2.97(N = 10\,000)$, $\alpha = -2.57(N = 3000)$, $\alpha = -2.54(N = 1000)$, and $\alpha = -2.15(N = 300)$.

[40] E. Tjhung and L. Berthier, Hyperuniform Density Fluctuations and Diverging Dynamic Correlations in Periodically Driven Colloidal Suspensions, Phys. Rev. Lett. **114**, 148301 (2015).